

# Palaeoenvironmental implications of Tertiary sediments from Kainan Maru Seamount and northern Gunnerus Ridge

CLAUS-DIETER HILLENBRAND<sup>1</sup> and WERNER EHRMANN<sup>2</sup>

<sup>1</sup>*Alfred Wegener Institute for Polar and Marine Research, PO Box 12 01 61, D-27515 Bremerhaven, Germany  
chillenbrand@awi-bremerhaven.de*

<sup>2</sup>*University of Leipzig, Institute for Geophysics and Geology, Talstrasse 35, D-04103 Leipzig, Germany*

**Abstract:** Sedimentary sequences spanning early Oligocene and Neogene time intervals were recovered with piston and gravity cores along erosional structures at northern Gunnerus Ridge and Kainan Maru Seamount in the southernmost Indian Ocean. Results of sedimentological investigations help to reconstruct the Cenozoic palaeoenvironment. Main emphasis was placed on grain size and clay mineral data. The clay mineral assemblages are dominated by illite and smectite. Chlorite and kaolinite occur in trace amounts. Whereas illite has a distinct source on the East Antarctic craton, smectite is of somewhat speculative origin, but probably is derived from erosion of Cenozoic or older shelf sediments. The presence of terrigenous sand indicates that ice-rafting was active throughout the time represented by the investigated cores, although with varying intensity. During the early Oligocene interval (30.1–29.0 Ma), siliceous phytoplankton production dominated sedimentation. Environmental conditions were quite different from those on Maud Rise and Kerguelen Plateau. The middle Miocene sedimentary sequence (14.1–12.8 Ma) documents an intensification of East Antarctic glaciation. The sediments deposited during the late Miocene interval (8.7–6.5 Ma) and the Pliocene interval (5.1–2.7 Ma) indicate continued cooling of Antarctica, but a more dynamic Antarctic ice sheet resulting in episodic sedimentation patterns.

Received 24 January 2003, accepted 15 July 2003

**Key words:** Antarctica, Cenozoic, clay minerals, glaciation, grain sizes, Southern Ocean

## Introduction

Sedimentologists, palaeontologists, palaeoclimatologists and palaeo-oceanographers expend much effort in reconstructing Cenozoic variations in the extent and volume of the Antarctic ice sheet, because these variations may be linked to global sea level, oceanic and atmospheric circulation patterns, and to major climatic changes (e.g. Bartek *et al.* 1996, Abreu & Anderson 1998, Barker *et al.* 1998, Zachos *et al.* 2001). In recent years, this has resulted in substantial progress in reconstructing Antarctic Cenozoic climatic and glacial history. Important contributions came from the Ocean Drilling Program (Legs 113, 114, 119, 177, 178, 188, and 189; Barker *et al.* 1990, Barron *et al.* 1991, Cisielski *et al.* 1991, Exon *et al.* 2001, O'Brien *et al.* 2001, Barker & Camerlenghi 2002, Gersonde & Hodell 2002) and other Antarctic drilling programmes, mainly the Cape Roberts Project (Hambrey *et al.* 1998, Barrett *et al.* 2000a, 2000b, 2001a, 2001b).

Many studies have concentrated on areas far from the Antarctic continent, because the sedimentary record there is relatively complete, and dating of the mainly pelagic sediments normally causes only minor problems due to a high content of microfossils. However, it is often difficult to decipher Antarctic climate and glacial history unambiguously from these records because of the possible interaction with climatic signals triggered farther to the north. The other main strategy is to study sediments

deposited directly from grounded or floating ice in proximal glaciomarine settings and glacial erosional features on the continental shelf. These sediments and features give clear evidence for ice advances and retreats through time, but the records are geographically restricted and often incomplete. Furthermore, dating problems due to a lack of microfossils and reworking of older sediments commonly limit the success of such studies. The same is true of onshore outcrops, which furthermore are rare.

This study attempts to bridge the gap between proximal and distal Antarctic marine records by analysing samples from Kainan Maru Seamount (KMS) and northern Gunnerus Ridge (GR) (Fig. 1a). Both structures are elevations in the southernmost Indian Ocean, rising more than 2000 m above the surrounding sea floor. The ridge system separates the bathyal areas of Cosmonaut Sea in the east from Riiser–Larsen Sea in the west. The GR stretches about 300 km northward off the Riiser–Larsen Peninsula, between 32°E and 36°E, to the south of KMS. KMS is detached from the northern GR by a narrow and deep depression (Fig. 1b). Thus, GR and KMS are close enough to the Antarctic continent that climatic changes in Antarctica and associated oceanographic changes in the Southern Ocean should have controlled the supply of terrigenous and biogenic components to these locations. During cruise ANT-VIII/6 of the RV *Polarstern* in 1990, several gravity and piston cores were taken from Neogene

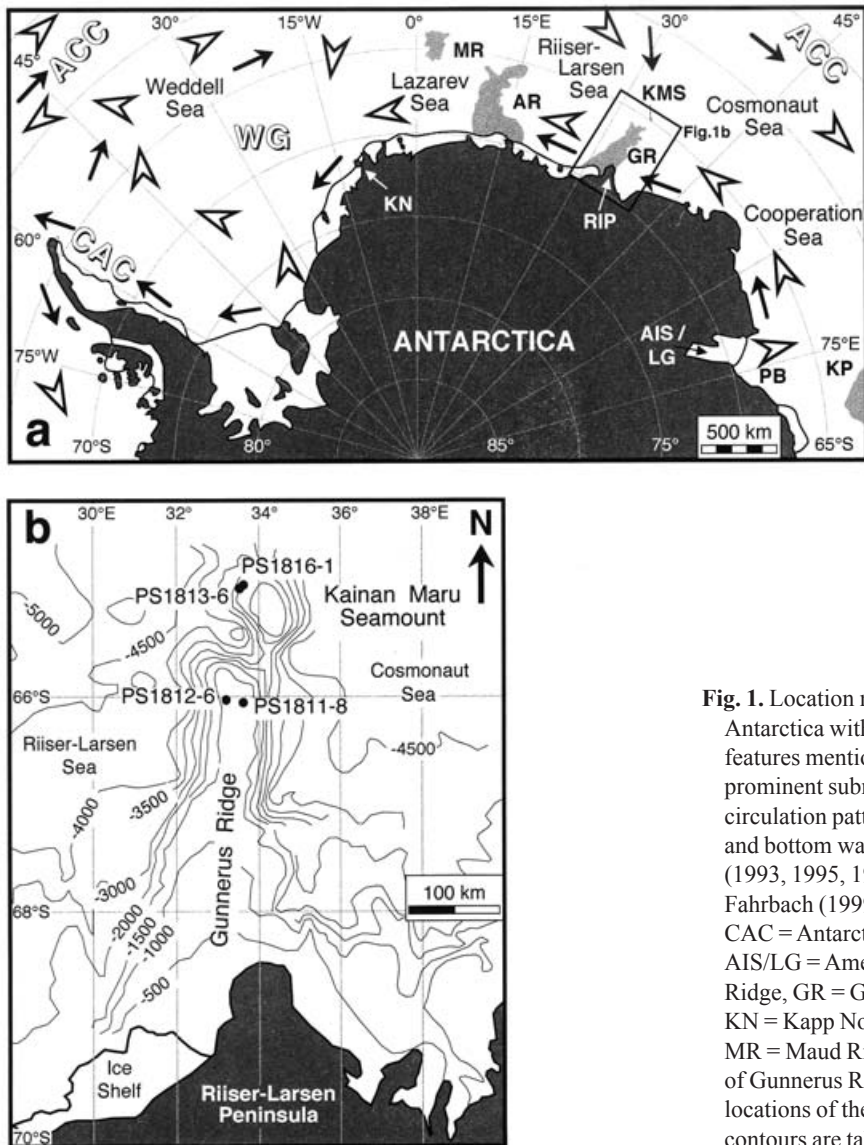


**Fig. 1.** Location map. **a.** The study area in the broader context of Antarctica with geographical locations and oceanographic features mentioned in the text. Ice shelves are shown white, prominent submarine topographic highs in grey. Schematic circulation patterns of surface waters (black arrows) and of deep and bottom waters (white arrows) were compiled after Orsi *et al.* (1993, 1995, 1999), Whitworth *et al.* (1998) and Schröder & Fahrbach (1999). ACC = Antarctic Circumpolar Current, CAC = Antarctic Coastal Current, WG = Weddell Gyre, AIS/LG = Amery Ice Shelf and Lambert Glacier, AR = Astrid Ridge, GR = Gunnerus Ridge, KMS = Kainan Maru Seamount, KN = Kapp Norvegia, KP = Kerguelen Plateau, PB = Prydz Bay, MR = Maud Rise, RIP = Riiser-Larsen Peninsula. **b.** Detail map of Gunnerus Ridge and Kainan Maru Seamount with the locations of the investigated sediment cores. Bathymetric contours are taken from Gersonde *et al.* (1998).

and Oligocene sediments excavated by large-scale slumps and slides (Fütterer & Schrems 1991). The water depth at the sampling sites ranged between *c.* 1150 m and 2200 m (Table I). The sediments consist mainly of diatom-bearing and/or radiolaria-bearing mud, siliceous mud, and diatom ooze. Therefore, they could be dated not only by magnetostratigraphy, but also by biostratigraphical means (Gersonde *et al.* 1998). The sedimentological work presented in this paper focussed on core sections, which were deposited during key periods of late Cenozoic Antarctic climate history (early Oligocene, middle Miocene, late Miocene and Pliocene) and not affected by disturbance or mass wasting.

### Oceanographic setting

The study area lies south of the eastward-flowing Antarctic Circumpolar Current (ACC), which affects the entire water

column and is driven by the westerly wind system. GR and KMS are overlain by the westward-flowing surface waters of the Antarctic Coastal Current (CAC) (Orsi *et al.* 1995), which merges with the southern branch of the Weddell Gyre (WG; Fig. 1a). The clockwise-flowing WG represents a prominent subpolar oceanographic feature between the Antarctic Peninsula and 20–30°E (Orsi *et al.* 1993, 1995, Schröder & Fahrbach 1999). Also on the continental slope and in the deep sea, ocean currents are directed to the west (Whitworth *et al.* 1998, Orsi *et al.* 1999). At these water depths GR and KMS are bathed by Circumpolar Deep Water (CPDW) and Antarctic Bottom Water (AABW). CPDW is the main water mass of the ACC, a mixture of bottom, deep and intermediate waters from the Atlantic, Pacific and Indian oceans (Emery & Meincke 1986). The very cold (0 to -0.7°C) AABW in the study area is thought to have been formed far to the east, in the vicinity of the Amery Ice Shelf (Orsi *et al.* 1999). During expeditions

**Table I.** Location and stratigraphical data of the investigated sediment cores.

Sediment core	Location	Latitude Longitude	Water depth (m)	Investigated depth range (m)	Age of investigated sediments	Samples
PS1811-8	northern Gunnerus Ridge	66°05.2'S 33°42.7'E	1147	0.4–2.7	late to early Pliocene <sup>1</sup> c. 4.4–2.7 Ma	26
PS1812-6	northern Gunnerus Ridge	66°03.8'S 33°16.9'E	1356	1.3–7.4	late Miocene to early Pliocene <sup>2</sup> 8.7–6.5 and 4.4–5.1 Ma	61
PS1813-6	Kainan Maru Seamount	64°57.2'S 33°38.1'E	2224	2.4–12.5	middle Miocene <sup>2</sup> 14.1–12.8 Ma	61
PS1816-1	Kainan Maru Seamount	64°55.2'S 33°42.8'E	2208	8.5–9.9	early Oligocene <sup>2</sup> 30.1–29.0 Ma	16

<sup>1</sup>Gersonde, in Fütterer & Schrems 1991<sup>2</sup>Gersonde *et al.* 1998

ANT-VIII/6 and ANT-XI/4, the boundary between AABW and CPDW was at a water depth of about 2300 m and 2000 m, respectively, off KMS (Fütterer & Schrems 1991, Schröder & Fahrbach 1999). The boundary rises to c. 1500 m water depth above the crest of GR. AABW and CPDW are overlain by a thin veneer of extremely cold Antarctic Surface Water (AASW).

### Material, methods and age models

For this study, we investigated Neogene and Oligocene sedimentary sections from cores PS1811-8, PS1812-6, PS1813-6, and PS1816-1 (Fig. 1b; Table I). About 10 cm<sup>3</sup> sample volume were taken at 10 cm intervals. For the

analysis of the grain-size distribution the sand fraction was isolated from the bulk sediment by sieving the samples through a 63 µm mesh. The clay fraction (< 2 µm) was separated from the silt fraction by the Atterberg method. The composition of the sand fraction was determined by point-counting terrigenous and biogenic particles under the microscope. Additionally, the results of the coarse-fraction analysis were multiplied with the sand content determined by grain-size separation in order to calculate the concentration of terrigenous sand within the bulk sediment.

For clay mineral analysis, 40 mg clay was dispersed in an ultrasonic bath and mixed with 1 ml of an internal standard consisting of a 0.04% MoS<sub>2</sub> suspension. The samples were mounted as texturally oriented aggregates by rapidly

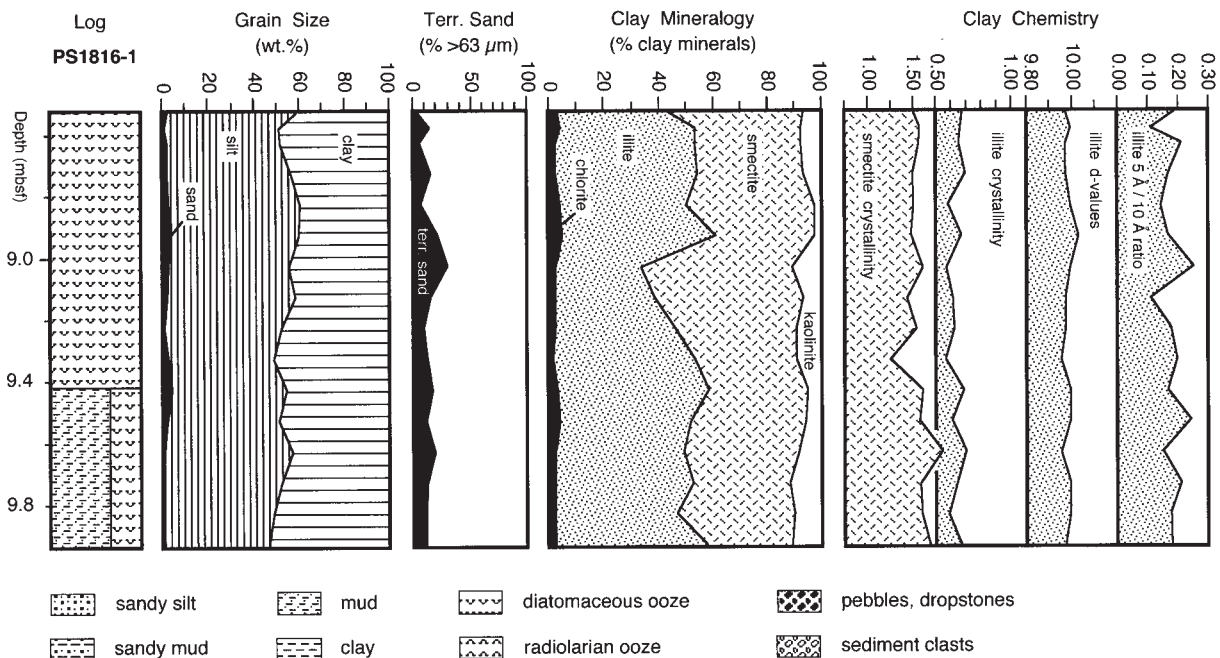


**Fig. 2.** Lithological log of the investigated sediments of core PS1816-1 (Fütterer & Schrems 1991), grain size data (sand, silt, clay; in wt.%), terrigenous components in the sand fraction (% > 63 µm), clay mineral composition (chlorite, illite, smectite, kaolinite; in % of clay minerals) and clay chemistry (smectite and illite crystallinities expressed as integral breadth values in  $\Delta^{\circ}2\theta$ , d-values in Å, and illite 5 Å/10 Å ratios).

**Table II.** Datums used for constructing the time scales for the investigated cores based on Fütterer & Schrems (1991) and Gersonde *et al.* (1998), using the time scale by Berggren *et al.* (1995). Linear sedimentation rates (LSR) are also given (LSR refers to the stratigraphical section underlying a particular age fix point).

Core	Depth (mbsf)	Age (Ma)	Datum	LSR (mm kyr <sup>-1</sup> )
PS1811-8	0.35	> 2.630	<i>F. interfrigidaria</i> / <i>T. insigna</i> zone	1.11
	1.65	3.800	Top <i>F. barronii</i> zone	1.73
	2.76	< 4.440	<i>F. barronii</i> zone	
PS1812-6	1.30	> 3.800	<i>F. barronii</i> zone	1.07
	1.35	4.480	Top C3n.2n	1.07
	1.50	4.620	Base C3n.2n	3.06
	2.05	4.800	Top C3n.3n	1.11
	2.15	4.890	Base C3n.3n	5.00
	2.60	4.980	Top C3n.4n	5.00
	3.29	< 5.230	<i>T. oestrupii</i> zone	
	3.29	> 6.269	<i>H. ovalis</i> zone	
	3.50	6.567	Base C3An.2n	1.90
	4.20	6.935	Top C3Bn	3.53
	4.75	7.091	Base C3Bn	2.27
	4.85	7.135	Top C3Br.1n	2.86
	4.95	7.170	Base C3Br.1n	1.35
	5.18	7.341	Top C3Br.2n	1.47
	5.23	7.375	Base C3Br.2n	2.11
5.35	7.432	Top C4n.1n	1.95	
6.60	8.072	Base C4n.2n	2.94	
7.05	8.225	Top C4r.1n	1.56	
7.10	8.257	Base C4r.1n	0.57	
7.35	8.699	Top C4An		
PS1813-6	2.30	> 12.840	<i>N. denticuloides</i> zone	7.28
	3.40	12.991	Top C5AAn	5.56
	4.20	13.135	Base C5AAn	1.20
	4.40	13.302	Top C5ABn	3.37
	5.10	13.510	Base C5ABn	13.14
12.54	< 14.076	C5ACn		
PS1816-1	8.46	> 28.350	<i>R. vigilans</i> zone	1.34
	9.00	29.401	Top C11n.1n	1.34
	9.35	29.662	Base C11n.1n	0.68
	9.42	29.765	Top C11n.2n	1.68
	9.98	< 30.098	C11n.2n	

filtering the suspension through a membrane filter. The filter cakes were dried at 60°C and mounted on aluminium tiles. They were exposed to ethylene glycol vapour at a temperature of 60°C for about 18 hr immediately before the X-ray analyses. The measurements were conducted on an automated powder diffractometer system Philips PW1700 with CoK $\alpha$  radiation (40 kV, 40 mA). The samples were X-rayed in the range 2–40°2 $\theta$  with a scan speed of 0.02°2 $\theta$  per second. Additionally, the range 28–30.5°2 $\theta$  was measured with a step size of 0.005°2 $\theta$  in order to better resolve the (002) peak of kaolinite and the (004) peak of chlorite. The X-ray diffractograms were evaluated on an Apple Macintosh Personal Computer using the “MacDiff” software (Petschick, freeware available from: <http://www.geologie.uni-frankfurt.de/staff/homepages/Petschick/Rainer.html#MacDiff>).

This study concentrates on the main clay mineral groups

**Table III.** Summary of grain size data and composition of the sand fraction for the sediment cores from Kainan Maru Seamount and Gunnerus Ridge

Core	Sand wt.% Range Mean SD	Silt wt.% Range Mean SD	Clay wt.% Range Mean SD	Terr. sand % > 63 $\mu$ m Range Mean SD	Terr. sand % in bulk sed. Range Mean SD	
PS1811-8	2–36 16 12.9	54–70 60 4.3	5–43 23 12.7	24–89 64 18.8	0–32 12 10.0	
	PS1812-6	0–43 14 10.9	37–72 58 6.9	11–56 28 12.1	31–94 75 15.9	0–27 10 7.8
		PS1813-6	2–21 7 4.0	44–64 54 4.1	25–50 39 5.8	1–63 16 17.0
PS1816-1			0–4 2 1.0	46–58 52 4.0	39–53 46 4.4	4–30 14 6.5

SD = standard deviation

smectite, illite, chlorite, and kaolinite. These clay minerals were identified by their basal reflections at ~17 Å (smectite), 10 and 5 Å (illite), 14.2, 7, 4.72, and 3.54 Å (chlorite), and 7 and 3.57 Å (kaolinite) (Ehrmann *et al.* 1992, Petschick *et al.* 1996). Semiquantitative evaluations of the mineral assemblages were made on the integrated peak areas. The relative percentages of smectite, illite, chlorite, and kaolinite were determined using empirically estimated weighting factors (Biscaye 1964, 1965, Brindley & Brown 1980). No effort was made to quantify mixed-layer clay minerals.

The crystallinity, a measure of the lattice ordering and crystallite size, is expressed as the integral breadth ( $\Delta^{\circ}2\theta$ ) of the smectite 17 Å peak and the illite 10 Å peak (Petschick *et al.* 1996). High values indicate poor crystallinities, low values indicate good crystallinities. Commonly used categories (cf. Petschick *et al.* 1996) for smectite crystallinities are: well crystallized (< 1.5  $\Delta^{\circ}2\theta$ ), moderately crystallized (1.5–2.0  $\Delta^{\circ}2\theta$ ), poorly crystallized (> 2.0  $\Delta^{\circ}2\theta$ ). Categories for illite crystallinities are: very well crystallized (< 0.4  $\Delta^{\circ}2\theta$ ), well crystallized (0.4–0.6  $\Delta^{\circ}2\theta$ ), moderately crystallized (0.6–0.8  $\Delta^{\circ}2\theta$ ), poorly crystalline (> 0.8  $\Delta^{\circ}2\theta$ ). The illite chemistry was inferred from the d-spacing (Å) of the 10 Å illite peak and from the 5 Å/10 Å peak-intensity ratio (e.g. Petschick *et al.* 1996). According to Esquevin (1969), 5 Å/10 Å ratios > 0.4 correspond to Al-rich illites (muscovite). The ratio decreases with Mg and Fe substituting the octahedral Al. Mg- and Fe-rich illites (biotite) have values < 0.15.

We used age models initially published by Fütterer & Schrems (1991) and Gersonde *et al.* (1998). The age models, which are based on magneto- and biostratigraphy, have been adjusted to the time scale of Berggren *et al.* (1995) (Table II). Linear sedimentation rates (LSR, in mm kyr<sup>-1</sup>) computed on the basis of these age models are

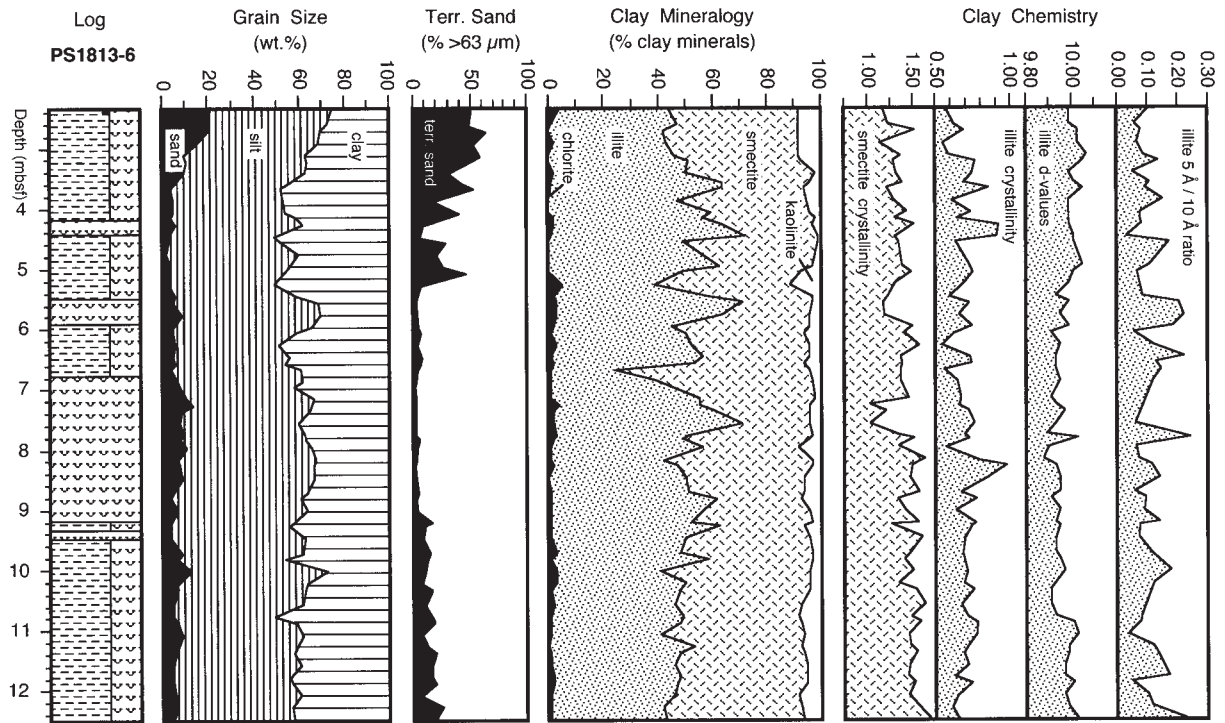


**Fig. 3.** Lithological log of the investigated sediments of core PS1813-6 (Fütterer & Schrems 1991), grain size data (sand, silt, clay; in wt.%), terrigenous components in the sand fraction ( $>63 \mu\text{m}$ ), clay mineral composition (chlorite, illite, smectite, kaolinite; in % of clay minerals) and clay chemistry (smectite and illite crystallinities expressed as integral breadth values in  $\Delta^{\circ}2\theta$ , d-values in Å, and illite 5 Å/10 Å ratios). For lithological legend see Fig. 2.

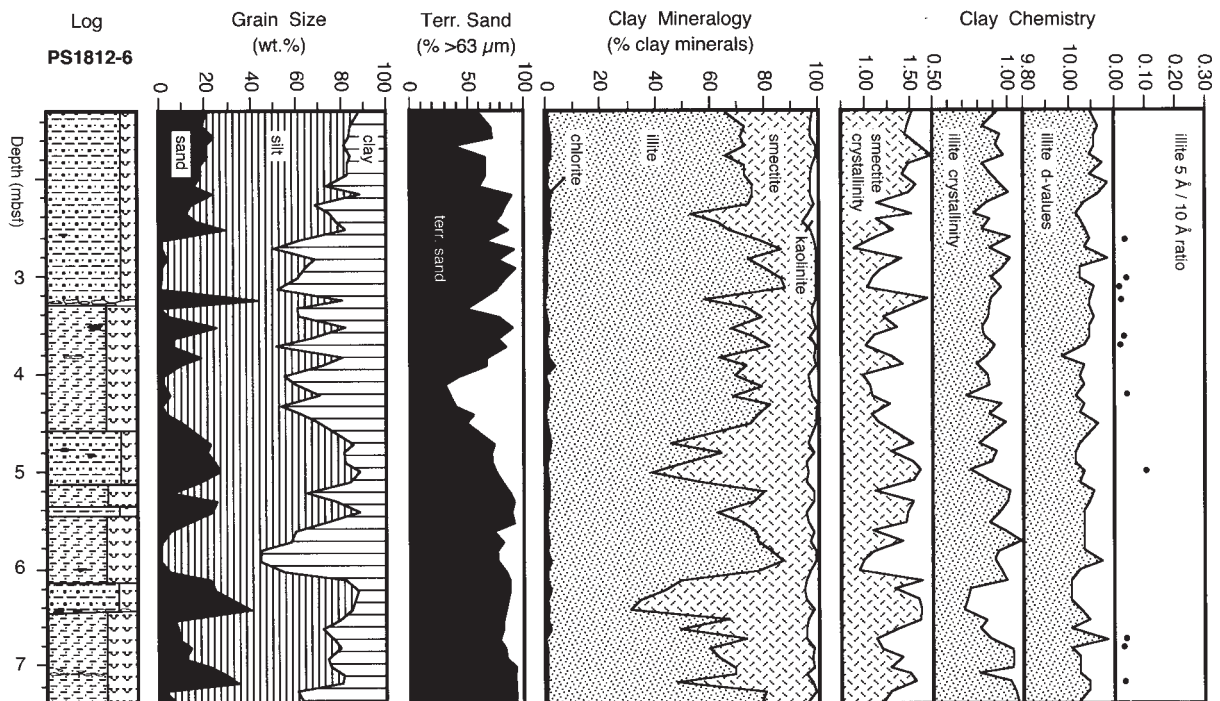


**Fig. 4.** Lithological log of the investigated sediments of core PS1812-6 (Fütterer & Schrems 1991), grain size data (sand, silt, clay; in wt.%), terrigenous components in the sand fraction ( $>63 \mu\text{m}$ ), clay mineral composition (chlorite, illite, smectite, kaolinite; in % of clay minerals) and clay chemistry (smectite and illite crystallinities expressed as integral breadth values in  $\Delta^{\circ}2\theta$ , d-values in Å, and illite 5 Å/10 Å ratios). For lithological legend see Fig. 2.

very low, ranging from about 1 to 13 mm kyr<sup>-1</sup> (Table II). Because of the different temporal resolution of the investigated sedimentary sequences, for better comparison the generated data sets were resampled at equal time increments of 80 kyr using the ANALYSERIES software (Paillard *et al.* 1996). All raw data are available via the data bank of the Alfred Wegener Institute for Polar and Marine Research, Bremerhaven, Germany (<http://www.pangaea.de/home/chillenbrand>).

## Results

The results of our sedimentological investigations are presented in Figs 2–5. They are summarized in Tables III and IV.

### Grain size distribution

The sand content in core PS1816-1 is consistently low and ranges between 0 and 4%, with a mean of 2% and a standard deviation of 1. This character is found similarly through most of core PS1813-6, though with a slightly higher mean value. However, at about 3.5 m below sea floor (mbsf) in this core the sand content rises steadily upwards to 21%. A totally different picture of highly variable sand content arises from cores PS1812-6 and PS1811-8, where values are in the range of 0–43% and 2–36%, respectively, mean

values of 14 and 16% and standard deviations of 11 and 13.

The concentration patterns of silt are very similar for cores PS1816-1 and PS1813-6, ranging from 46 to 58% in the former and from 44 to 64% in the latter. The mean values are 52% and 54% respectively, the standard deviation is 4.0 in both cores. Slightly higher silt concentrations can be observed in the other cores, with a range of 37–72% and a mean of 58% in core PS1812-6, and a range of 54–70% and a mean of 60% in core PS1811-8. The standard deviations are 6.9 and 4.3, respectively. The clay content shows a trend opposite to that of the sand content. In core PS1816-1 silt contents only slightly fluctuate around a relatively high value of 46%. A similar pattern dominates the lower part of core PS1813-6, while in the uppermost part the concentrations decrease to 25%. In both core PS1812-6 and core PS1811-8 the standard deviation (12.1 and 12.7) is higher than in the other two cores (4.4 and 5.8).

### Composition of the sand fraction

The sand fraction of the investigated sediments contains terrigenous debris (mainly quartz and feldspar) and siliceous particles (remains of radiolaria and diatoms). Because of the complexity between production and deposition of biogenic opal, which is influenced by various processes of dissolution and preservation (e.g. Ragueneau

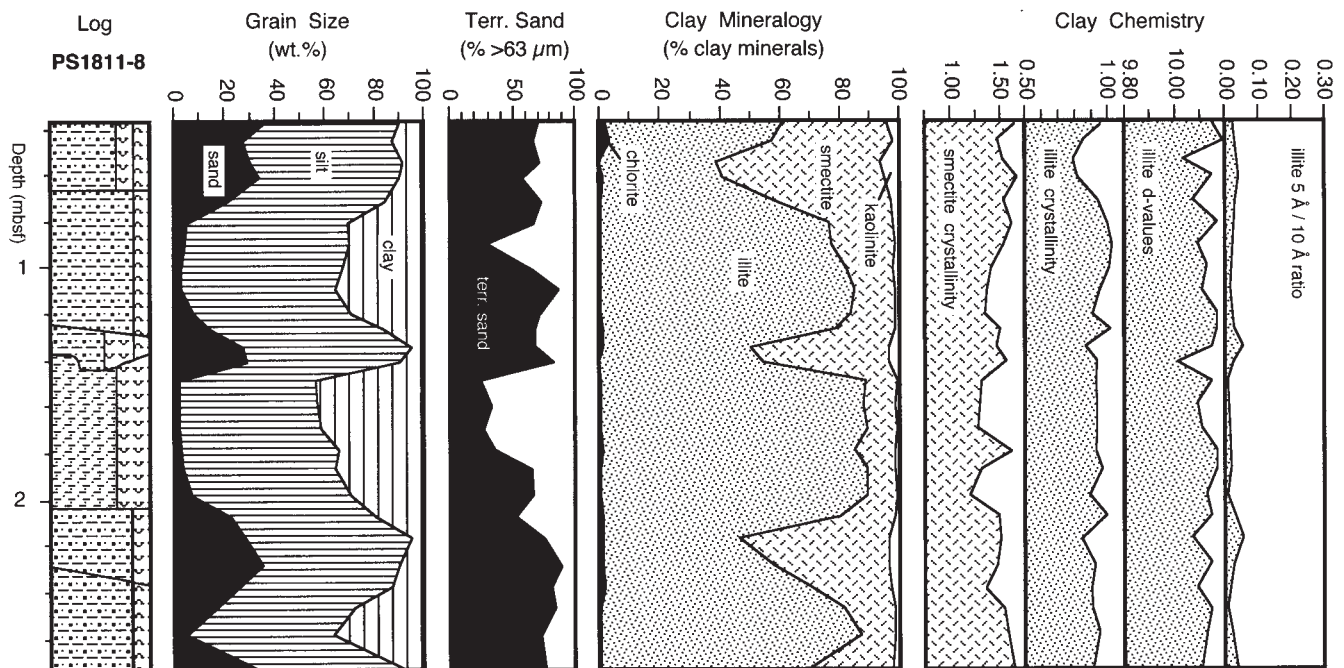


**Fig. 5.** Lithological log of the investigated sediments of core PS1811-8 (Fütterer & Schrems 1991), grain size data (sand, silt, clay; in wt.%), terrigenous components in the sand fraction (% > 63 μm), clay mineral composition (chlorite, illite, smectite, kaolinite; in % of clay minerals) and clay chemistry (smectite and illite crystallinities expressed as integral breadth values in  $\Delta^{\circ}2\theta$ , d-values in Å, and illite 5 Å/10 Å ratios). For lithological legend see Fig. 2.

*et al.* 2000), in this paper we consider only the terrigenous sand components. In core PS1816-1, 4–30% of the sand fraction consists of terrigenous detritus (mean 14%). Very similar values are found in the lower part of core PS1813-6. In the upper part, above 5.2 mbsf, the content of terrigenous sand increases to 50–60%. Even higher values, with a mean of 75%, occur in core PS1812-6. However, minimum values down to 30% are found at 4.0 to 4.5 mbsf. A range between 24 and 89% (mean 64%) is observed in core PS1811-8.

*Clay mineralogy*

Smectite concentrations vary between 32 and 56% in core PS1816-1 and between 25 and 71% in core PS1813-6. The mean values are 42% and 43%, the standard deviations 6.8 and 8.1, respectively. The sediments of the other two cores show generally lower smectite concentrations of 11–67% with a mean of 29% in PS1812-6, and concentrations of 9–55% with a mean of 26% in PS1811-8. The stronger variability in these two cores finds expression in higher standard deviations of 12.4 and 15.1, respectively. The crystallinity of the smectites as expressed by the values of integral breadth (high values indicate poor crystallinity) ranges between 1.0 and 1.8  $\Delta^{\circ}2\theta$ , with mean values of 1.55  $\Delta^{\circ}2\theta$  in PS1816-1, 1.41  $\Delta^{\circ}2\theta$  in PS1813-6, 1.33  $\Delta^{\circ}2\theta$  in PS1812-6 and 1.47  $\Delta^{\circ}2\theta$  in PS1811-8. Thus, the investigated smectites belong mainly to the category of well crystallized smectites ( $< 1.5 \Delta^{\circ}2\theta$ ) and, less commonly, to the category of moderately crystallized smectites (1.5–2.0  $\Delta^{\circ}2\theta$ ).

Illite shows a concentration pattern opposite to that of smectite. As for smectite concentration, similarity exists between cores PS1816-1 and PS1813-6, and between cores PS1812-6 and PS1811-8. The mean concentrations in the former two cores are 48% and 59%, in the latter two cores

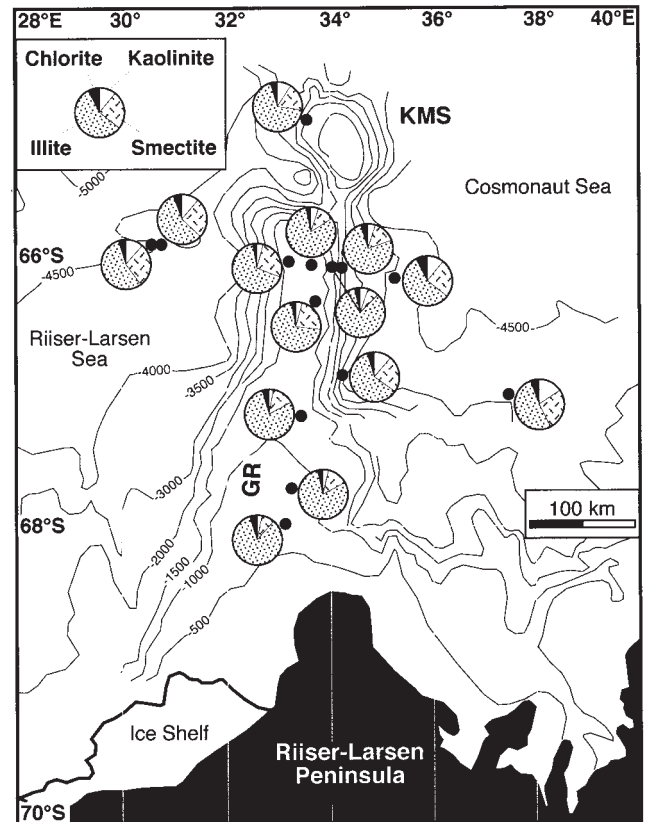


**Fig. 6.** Clay mineral assemblages in surface sediment samples recovered in the area of Gunnerus Ridge and Kainan Maru Seamount (data taken from Petschick *et al.* 1996).

68% and 71%. In PS1816-1 and in the lower part of PS1813-6 the d-values of illite are  $< 10.0 \text{ \AA}$  and therefore indicate a muscovitic composition. However, the 5  $\text{Å}/10 \text{ \AA}$  ratios are mainly 0.10–0.25 and suggest a composition between Al-rich (muscovite) and Mg- and Fe-rich (biotite)

**Table IV.** Summary of clay mineral data for the sediment cores from Kainan Maru Seamount and Gunnerus Ridge.

Core	Illite % clay min. Range Mean SD	Chlorite % clay min. Range Mean SD	Kaolinite % clay min. Range Mean SD	Smectite % clay min. Range Mean SD	10 $\text{Å}$ Illite d-value ( $\text{Å}$ ) Range Mean SD	Illite cryst. $\Delta^{\circ}2\theta$ Range Mean SD	Illite 5 $\text{Å}/10\text{Å}$ Range Mean SD	Sm. cryst. $\Delta^{\circ}2\theta$ Range Mean SD
PS1811-8	39–89 71 16.5	0–4 1 0.8	1–6 2 1.4	9–55 26 15.1	10.011–10.189 10.12 0.04	0.8–1.0 0.93 0.06	0.0–0.06 0.03 0.01	1.2–1.7 1.47 0.13
PS1812-6	30–87 68 13.2	0–3 1 0.7	0–6 3 1.4	11–67 29 12.4	9.972–10.169 10.07 0.04	0.7–1.1 0.91 0.09		0.9–1.8 1.33 0.22
PS1813-6	23–71 50 8.6	0–5 2 1.1	1–12 5 2.1	25–71 43 8.1	9.877–10.070 9.97 0.04	0.5–1.0 0.70 0.09	0.0–0.24 0.11 0.05	1.0–1.7 1.41 0.14
PS1816-1	31–56 48 7.0	2–5 3 1.0	2–12 8 2.7	32–56 42 6.8	9.953–10.031 9.98 0.02	0.6–0.7 0.64 0.05	0.1–0.3 0.18 0.04	1.3–1.8 1.55 0.12

SD = standard deviation

(Esquevin 1969). In the upper part of PS1813-6 and in PS1812-6 and PS1811-8, the *d*-values are generally  $> 10.0 \text{ \AA}$ , typical for biotitic illites. The  $5 \text{ \AA}/10 \text{ \AA}$  ratios are  $< 0.15$  and clearly also indicate biotitic nature of the illites. The illite integral breadth shows also a compositional difference between sediments of the two cores PS1816-1 (mean  $0.7 \Delta^{\circ}2\theta$ ) and PS1813-6 (mean  $0.6 \Delta^{\circ}2\theta$ ) and the other two cores PS1812-6 (mean  $0.9 \Delta^{\circ}2\theta$ ) and PS1811-8 (mean  $0.9 \Delta^{\circ}2\theta$ ). The investigated illites hence belong to the moderately crystallized and the poorly crystallized groups.

Chlorite occurs in trace amounts of 0–5% in all investigated cores. Mean concentration is 3% in PS1816-1, 2% in PS1813-6, and 1% in cores PS1812-6 and PS1811-8. Kaolinite concentrations in the four cores are 0–12%, with mean values of 8% in PS1816-1, 5% in PS1813-6, 3% in PS1812-6 and 2% in PS1811-8.

## Discussion

### *Sources for coarse terrigenous matter*

The terrigenous coarse fraction of the sediments recovered at northern GR and KMS consists mainly of quartz and feldspar grains and is believed largely to represent ice-rafted debris (IRD). IRD is delivered to the distal marine environment by icebergs calving from ice streams and outlet glaciers into the sea (e.g. Anderson 1999). IRD has all grain-size classes represented in roughly equal parts (Drewry 1986), but clay and silt fractions of sediments are also subject to a variety of other transport processes. Therefore, most studies use only the concentration of terrigenous sand or gravel as a measure of the ice-rafting intensity (e.g. Grobe & Mackensen 1992, Diekmann & Kuhn 1999). In this paper, we use the concentration of the terrigenous sand fraction as an indicator for ice rafting. This seems reasonable, because the sample sites are on top of long lived submarine elevations that cannot have been reached by turbidity currents. Moreover, the terrigenous sand content of the sediments correlates with the abundance of gravel grains counted on X-ray slabs (Grobe, unpublished data), which is also used as a proxy for IRD.

### *Sources for the clay minerals*

Within the study area, Petschick *et al.* (1996) investigated 14 surface sediment samples, which are assumed to result from late Pleistocene to Holocene deposition considering the age models for the core tops taken from the same locations (Gersonde *et al.* 1998). The authors found 52–84% illite, 7–28% smectite, 3–16% kaolinite, and 3–7% chlorite (Fig. 6). Thus, the clay mineral distribution in the surface sediments is similar to the late Miocene and Pliocene clay mineral assemblages of sites PS1811 and PS1812 on northern GR, but characterized by generally lower smectite contents. In the surface sediments, crystallinities of smectite vary between  $0.9$  and  $2.0 \Delta^{\circ}2\theta$

and crystallinities of illite range from  $0.6$  to  $0.8 \Delta^{\circ}2\theta$ , with *d*-values  $> 10.06 \text{ \AA}$  and  $5 \text{ \AA}/10 \text{ \AA}$  ratios  $< 0.1$  (Petschick *et al.* 1996). This chemical composition of the smectites and illites corresponds to that in the Tertiary sediments on northern GR and KMS.

### Illite

In the Atlantic sector of the Southern Ocean, high illite concentrations (up to 84%) are reported from surface sediments both on the southern GR and along the East Antarctic continental margin, suggesting a source in the East Antarctic hinterland (Petschick *et al.* 1996). Illite is a detrital clay mineral and derives from crystallized rocks, which are widespread on the East Antarctic craton (Tingey 1991a, 1991b). The biotite-bearing, highly metamorphic rocks in particular may serve as a source (cf. Gingele *et al.* 1997, Diekmann & Kuhn 1999). In a glacial regime, the otherwise relatively unstable biotitic illites preserve their chemical and structural properties instead of being broken down to other clay minerals (Petschick *et al.* 1996).

### Chlorite

Chlorite occurs only in trace amounts in the investigated Tertiary sediments. Chlorite is likewise uncommon in the surface sediments of the Atlantic sector of the Southern Ocean. Higher concentrations (up to 30%) are restricted to only a few Antarctic shelf areas (Petschick *et al.* 1996). Chlorite, representing a detrital clay mineral, is typically derived from the weathering of low-grade, chlorite-bearing metamorphic and basic rocks as are commonly found in East Antarctica (Tingey 1991a, 1991b).

### Kaolinite

Kaolinite cannot form under polar conditions, because it is a product of chemical weathering, characteristic of moist, temperate to tropical regions. However, kaolinite may be found as a recycling product also in polar environments because of its resistance to physical erosion (e.g. Ehrmann *et al.* 1992). The surface distribution of kaolinite in the Atlantic sector of the Southern Ocean exhibits a tongue extending from the Indian Ocean sector to Maud Rise, thereby passing GR, KMS, and Astrid Ridge (Petschick *et al.* 1996). Such distribution reflects the westward transport by ocean currents.

The source area for the kaolinite is still under debate. Kaolinite may be derived from the weathering of sediments of the Permo–Triassic Amery Group in the northern Prince Charles Mountains upstream of the Amery Ice Shelf/Lambert Glacier system, or from recycling products of these sediments in the same region (e.g. the Cenozoic Battye Glacier and Bardin Bluffs formations; Ehrmann *et al.* 2003). Clay mineral assemblages in Holocene sediments recovered from the shelf west of the Amery Ice Shelf are dominated by kaolinite (Harris & O'Brien 1998). Gingele *et al.* (1997) and Petschick *et al.* (1996) assume kaolinite-bearing Palaeogenic sediments cropping out at

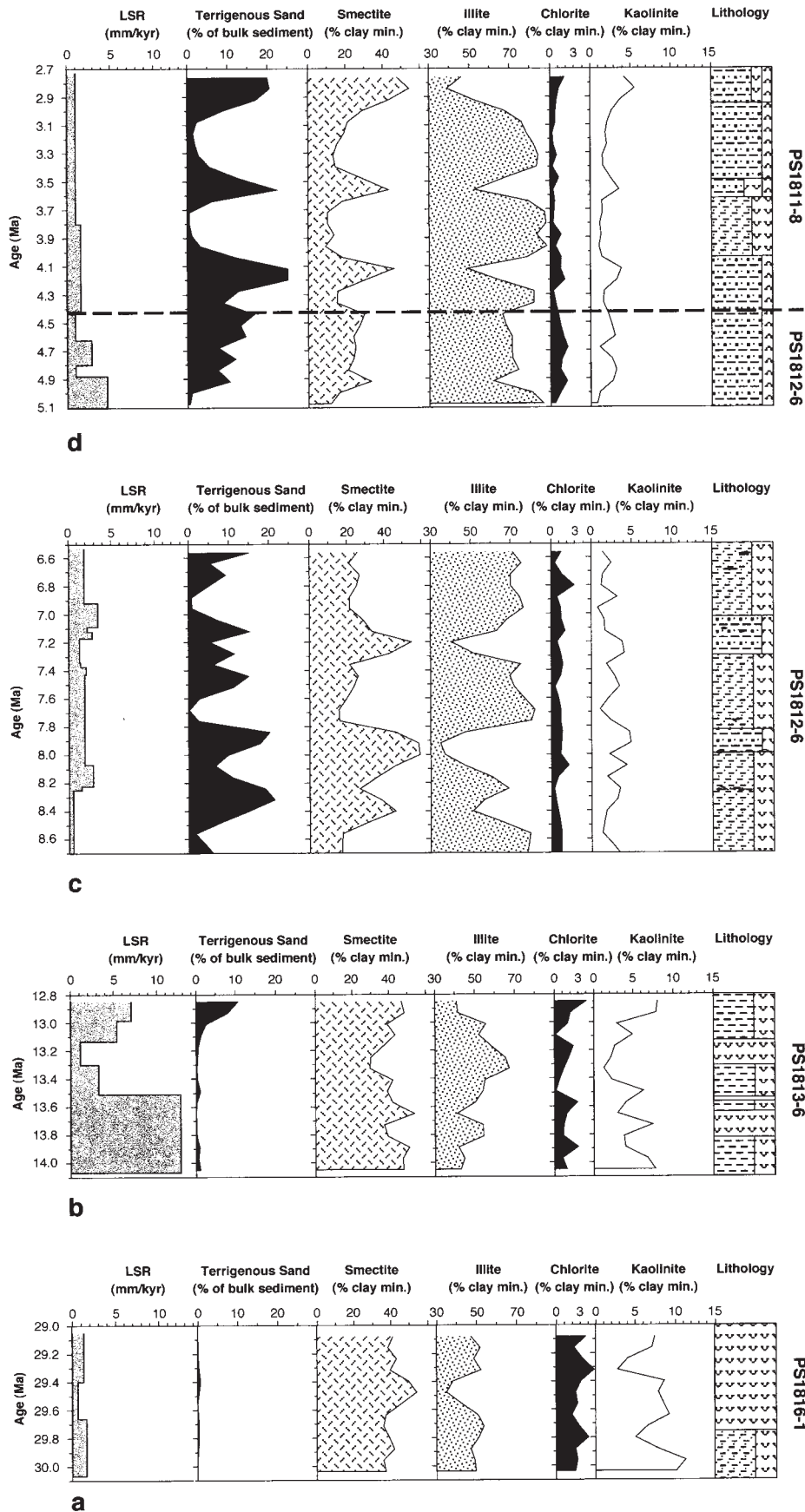


**Fig. 7.** Main sedimentological parameters determined in the sediment cores from northern Gunnerus Ridge and Kainan Maru Seamount plotted versus age: linear sedimentation rates (LSR, in  $\text{mm kyr}^{-1}$ ), percentage of terrigenous sand in the bulk sediment, and percentages of smectite, illite, chlorite and kaolinite.

submarine ridges, like Maud Rise, as additional possible sources. However, because of the westward current regime in the study area, we suggest that kaolinite is mainly supplied from source rocks located close to the Amery Ice Shelf. In surface sediments, kaolinite contents exceeding 10% are confined to the flanks of GR below 3000 m water depth (Fig. 6). In the Lazarev Sea, located west of the Riiser–Larsen Sea, enhanced kaolinite concentrations are also restricted to such large water depths (Gingele *et al.* 1997). Therefore, we assume a current-induced kaolinite supply by the “Antarctic Slope Current” (Whitworth *et al.* 1999) and/or by westward AABW advection (Orsi *et al.* 1999) rather than by the CAC.

### Smectite

The smectite concentrations in the surface sediments of northern GR and KMS are significantly lower than in the Tertiary sequences from the same area (Fig. 6; Results). During the present interglacial, high concentrations of smectite are mainly confined to volcanic areas in the Atlantic Sector of the Southern Ocean, such as the South Sandwich Islands, Maud Rise, and the Atlantic–Indian Mid-Ocean Ridge system (Petschick *et al.* 1996, Diekmann *et al.* 1999). The smectites in these areas are nontronites (Fe-rich smectites), which are characterized by integral breadth values of  $< 1.5 \Delta^{\circ}2\theta$  and which are thought to have been generated from the alteration of basaltic rocks and volcanic glass undergoing submarine weathering (Petschick *et al.* 1996). GR and KMS themselves consist of continental crust (Roeser *et al.* 1996). Therefore, their basement rocks are unlikely sources for smectite, although the overlying Tertiary strata may be an important source (Gingele *et al.* 1997, this paper).

High contents of well crystallized smectites are also common along the continental slope off Kapp Norvegia, possibly indicating weak chemical weathering of mafic intrusive and volcanic source rocks in the East Antarctic hinterland (Ehrmann *et al.* 1992, Petschick *et al.* 1996). Alternatively, erosion of smectite-enriched, pre-glacial Mesozoic and Cenozoic strata cropping out on the shelf (Robert & Maillot 1990) may cause increased smectite concentrations in the surface sediments off Kapp Norvegia. Spatial distribution of smectite and kaolinite in surface sediments recovered in the Lazarev Sea suggests a common source (Gingele *et al.* 1997). In the study area, however, the spatial distribution of smectite in the surface sediments exhibits no relation to water depth like kaolinite (see above; Fig. 6), and thus the hypothesis of a common source must be excluded.

Exclusively considering the present spatial distribution of smectite sources, only significant changes in the oceanographic circulation pattern may explain the high smectite contents in the Tertiary sediments on GR and KMS. Smectite delivery from the Atlantic–Indian Ridge system requires a southward directed current, e.g. a south-

eastward extension of the WG. This pathway is conceivable, because significant volumes of water derived from the ACC can be transported to the areas just north and east of KMS by mesoscale eddy fields (Schröder & Fahrbach 1999). According to Orsi *et al.* (1993), the water mass advected from the ACC into the eastern WG is CPDW originating from North Atlantic Deep Water (NADW), which theoretically could have swept the smectite-rich volcanogenic sediments on the south-west Indian Ridge. However, Diekmann *et al.* (1999) observed no exchange of clay minerals between the ACC and the WG to the west of the study area throughout the late Quaternary. Moreover, because the KMS and GR effectively constrain the position of the WG (Schröder & Fahrbach 1999), it is unlikely that the WG is able to advect associated water masses above the two topographic highs.

On the other hand, smectite supply from Kapp Norvegia requires an eastward current, e.g. a southward shift of the ACC by more than  $10^{\circ}$  of latitude. The ACC exists since about 33 Ma (Latimer & Filipelli 2002). A (Proto-)WG probably existed already in the early Oligocene, but might have affected exclusively surface water masses (Mackensen & Ehrmann 1992). The first indications for a (Proto-)WG, which influenced the deep- and bottom-water circulation, and thus for a WG, which was able to prevent the southward transport of terrigenous detritus derived from the ACC (cf. Diekmann *et al.* 1999), dates back to the early to late Miocene (Pudsey 2002, Michels *et al.* 2002). Therefore, only the high smectite contents found in the lower Oligocene sediments on KMS could be explained by smectite delivery from Kapp Norvegia. Because of these discrepancies, we suppose smectite supply from either the Atlantic–Indian Ridge system or Kapp Norvegia to GR and KMS to be unlikely even during the past.

Smectite concentrations comparable to those observed in the Tertiary strata on GR and KMS were also reported from Oligocene to Pliocene sedimentary sequences drilled in the eastern Weddell Sea (Robert & Maillot 1990). The relatively high smectite contents were traced back to the glacial erosion and reworking of pre-glacial Cenozoic and Mesozoic shelf sediments in East Antarctica, which bear significant amounts of smectite (Robert & Maillot 1990). Following this suggestion, we assume that smectite was delivered to GR and KMS by the reworking of such “old” shelf sediments outcropping somewhere to the east of the study area. These sources must have played a more important role during the Tertiary than today.

### The palaeoenvironmental record

Although the investigated sections of the four cores from northern GR and KMS cannot be combined to a continuous stratigraphic record (Table I, Fig. 7), some trends in the Tertiary development of the palaeoenvironment can be identified.

### Early Oligocene

The sedimentary record of core PS1816-1 spans the time interval 30.1 to 29.0 Ma (Fig. 7a), and thus a part of the late early Oligocene. It begins after the establishment of continental glaciation in East Antarctica some 33 Ma ago (e.g. Ehrmann & Mackensen 1992, Lear *et al.* 2000, Zachos *et al.* 2001), which is assumed to coincide with the opening and deepening of Drake Passage and of the Tasmanian Gateway (Exon *et al.* 2001, Lawver & Gahagan 2003). Very low concentrations of terrigenous sand in the diatomaceous muds and oozes (Fig. 2) indicate ice rafting, but not as a major process. This agrees with previous observations from Maud Rise and Kerguelen Plateau, showing that the concentrations of IRD had declined drastically after a sharp and intense pulse of ice rafting accompanying the onset of continental glaciation in the earliest Oligocene (Wise *et al.* 1991, Ehrmann & Mackensen 1992).

The sedimentation of diatomaceous muds and oozes on KMS during the early Oligocene contrasts with the synchronous deposition of calcareous oozes on Maud Rise (ODP sites 689, 690) and on the southern Kerguelen Plateau (ODP sites 738, 744) located at similar latitudes (*c.* 65° and 62°, respectively) (Barron *et al.* 1989, Barker *et al.* 1988). In the recent Southern Ocean, calcareous nannofossil oozes dominate north of the Polar Front, whereas diatomaceous oozes dominate between the Polar Front and the summer sea-ice limit (Burckle & Cirilli 1987). Therefore, the nature of biogenic sedimentation can be used to reconstruct palaeoceanography (e.g. Burckle *et al.* 1996). The deposition of biosiliceous sediments on KMS can be explained by relatively low surface water temperatures inhibiting primary production of calcareous phytoplankton, dissolution of calcareous microfossils, and/or by a dominance of diatom production in response to cool-water upwelling. The upwelling may have resulted from intense wind stress caused by ice build-up on the Antarctic continent (cf. Kennett & Barker 1990).

Thus, the early Oligocene occurrence of biosiliceous sediments with very low IRD contents on KMS suggests that surface water temperatures were high enough to melt most icebergs and sea ice south of site PS1816, but low enough to favour primary production of siliceous phytoplankton. The contrast between the depositional styles on KMS on one hand, and on Maud Rise and Kerguelen Plateau on the other hand may result from the development of a (Proto-)WG off Dronning Maud Land (Mackensen & Ehrmann 1992) and of a cold coastal surface current similar to the modern CAC off Prydz Bay, respectively (Wei & Wise 1990). These current systems may have separated cold and warmer surface water regimes (Mackensen & Ehrmann 1992) and caused different styles of phytoplankton production.

In the lower Oligocene sediments of core PS1816-1, illite and smectite occur in similar proportions, which probably indicates the reworking of pre-glacial smectite-bearing

deposits from the Antarctic shelf and a dilution of the illite derived from the East Antarctic hinterland. A general decrease of kaolinite pointing to a gradual removal of “old” sediments from the shelf corroborates this hypothesis. We exclude the possibility that the weathering conditions in the early Oligocene still formed significant amounts of pedogenic clay minerals. Elsewhere on the East Antarctic continental margin clay mineral assemblages document the dominance of physical weathering at this time (e.g. Ehrmann & Mackensen 1992, Robert & Kennett 1997).

The early Oligocene fluctuations in clay mineralogy and grain size on KMS were less pronounced than during the following Neogene period. The sedimentation rates were almost constant. This suggests the prevalence of relatively stable environmental conditions in Antarctica and the adjacent Southern Ocean.

### Middle Miocene

The middle Miocene sedimentary sequence of core PS1813-6 (Fig. 7b) ranges from 14.1 to 12.8 Ma. Within the 14.1 to 13.5 Ma old diatomaceous clay and ooze, the amount of IRD is very low. Smectite and kaolinite decrease slightly with time at the expense of illite. This sediment composition points to environmental conditions similar to those of the early Oligocene.

In the diatomaceous clay and ooze deposited on KMS between 13.5 and 13.1 Ma, IRD is generally lacking, too, but contents of illite are high and the linear sedimentation rates are quite low. We interpret these sediments to be deposited under relatively warm climatic conditions, south of the Polar Front. The relatively warm surface water temperatures prevented icebergs reaching KMS. Grounded ice masses on the Antarctic continent probably had retreated far to the south. Thus, glacial reworking of smectite-enriched shelf sediments was less active, and only low amounts of fine-grained terrigenous detritus from the adjacent East Antarctic hinterland were supplied to KMS by waves and tidal currents. Particularly, the diatom ooze, which was deposited between 13.31 and 13.13 Ma with a very low sedimentation rate, obviously represents a condensed section with strongly reduced terrigenous input.

From 13.1 to 12.8 Ma the IRD content increased unprecedentedly, accompanied by a slight decrease of illite at the expense of smectite and kaolinite. Diatomaceous clays with high contents of terrigenous detritus were deposited on KMS with increasing sedimentation rates. We interpret this change in deposition style to be caused by enhanced ice discharge along the coasts resulting in a generally higher delivery of terrigenous detritus and increased iceberg supply. Cooling of the surface waters in the Southern Ocean allowed more icebergs reaching KMS. The increase of the smectite and kaolinite contents resulted from the intensified erosion of shelf sediments by grounded ice masses. These ice masses advanced across the East Antarctic shelf as a consequence of sea-level drop in

response to ice sheet build-up in Antarctica.

The palaeoenvironmental record on KMS agrees well with conclusions from the global sea-level curve and the benthic foraminiferal oxygen isotope record. These indicate that the middle Miocene was characterized by a climatic optimum followed by a step-like growth of ice masses between *c.* 15 and 13 Ma that affected both East and West Antarctica (Flower & Kennett 1994, Abreu & Anderson 1999, Lear *et al.* 2000, Zachos *et al.* 2001, Barker & Camerlenghi 2002, Billups & Schrag 2002). A major ice sheet had re-established in Antarctica by 13 Ma (Zachos *et al.* 2001), but estimates of absolute ice volume during that time interval are uncertain (Billups & Schrag 2002).

#### Late Miocene

A major change in the composition of the clay mineral assemblages occurred between the deposition of the sediments at site PS1813 on KMS and site PS1812 on GR, *i.e.* between some 12.8 and 8.5 Ma (Fig. 7b & c). Compared to the middle Miocene the mean concentration of illite is *c.* 20% higher, whereas that of smectite is about 15% lower. In the upper Miocene diatom-bearing muds of core PS1812-6 also the kaolinite content is slightly lower than in the middle Miocene sediments of core PS1813-6. The illite chemistry had changed as well pointing to source rocks enriched in biotite. At present, clay mineral assemblages deposited on northern GR and KMS above the CPDW/AABW boundary are very similar (Fig. 6). Therefore, the clay mineralogical shift observed between 12.8 and 8.5 Ma is unlikely to represent simply an effect of distance from the Riiser-Larsen Peninsula. Moreover, the clay mineralogical shift from the middle Miocene to the late Miocene involved a further increase of IRD (Fig. 7b & c).

These sedimentological changes probably reflect continued cooling in Antarctica. During the late Miocene, additional climatic deterioration had triggered further ice sheet expansion and formation of large ice shelves in Antarctica (Kennett & Barker 1990, Zachos *et al.* 2001). The clay mineral assemblage deposited between 8.7 and 6.5 Ma on GR suggests that a dry polar weathering regime had ultimately established in the East Antarctic source areas, and that smectite-enriched, kaolinite-bearing, preglacial strata had largely been removed from the nearby East Antarctic continental shelf. The relatively high rates of IRD deposition on GR probably resulted from cooling of the Southern Ocean surface waters in combination with higher iceberg supply from the hinterland triggered by continued ice sheet growth since the middle Miocene. Surface water cooling during the late Miocene enabled icebergs to transport IRD to distant regions as far as the subantarctic Indian and Atlantic oceans (Ehrmann *et al.* 1991, Breza 1992, Warnke *et al.* 1992).

The variations of the sedimentological parameters in core PS1812-6 (and also in core PS1811-8) are much more pronounced than in the other two cores (Fig. 7, Tables III &

IV), suggesting that the late Miocene cooling trend was superimposed by short-term climatic fluctuations. On northern GR, diatomaceous mud, which tends to bear relatively low contents of well-crystallized smectite, alternates with diatom-bearing sandy mud, which tends to contain higher concentrations of less crystallized smectite. This depositional pattern documents that starting from the late Miocene, when the smectite-rich strata on the adjacent shelf had been eroded away, smectite-enriched terrigenous debris rather was delivered from distal sources by icebergs, whereas illite-enriched detritus derived from the Riiser-Larsen Peninsula preferentially was supplied by waves and tidal currents. This hypothesis is corroborated by the co-occurrence of maxima in smectite and IRD contents during late Quaternary interglacial periods, which is reported from a sedimentary sequence recovered from the eastern flank of GR (Diekmann *et al.* in press). Consequently, we assume that the relatively IRD-poor sediments on GR were deposited during colder periods, when perennial sea ice coverage effectively hampered the drift of icebergs.

Thus, the generally increased concentrations of IRD and illite after 8.7 Ma obviously indicate stronger glacial conditions in Antarctica on a long-term time scale, whereas the superimposed maxima of IRD and smectite represent short-term interglacial conditions of a second order. The fact, that the clay mineralogy and the IRD concentrations on GR exhibited more distinct variations after 8.7 Ma than before 12.8 Ma may point to a more dynamic Antarctic ice sheet on time scales, which may range on the order of Milankovitch cycles. However, these ice sheet fluctuations need not necessarily to be driven by orbital parameters (Barker *et al.* 1999, Barker & Camerlenghi 2002).

#### Pliocene

From a long-term perspective, the terrigenous sand and clay mineral contents in the sediments of core PS1811-8 seem to reflect climatic conditions similar to those of the late Miocene (Fig. 7d). During the Pliocene, clay mineral composition and IRD record show even more pronounced short-term variations in respect to the late Miocene. At site PS1811, an episodic depositional pattern is observed between 4.4 and 2.7 Ma. Fine-grained and illite-enriched radiolarian- and diatom-bearing muds, which we suppose to be deposited under more glacial climatic conditions, clearly alternate with smectite-enriched siliceous muds bearing high concentrations of IRD, which we assume to reflect interglacial conditions. It is well known that during the Pliocene the Antarctic ice sheets experienced frequent volume changes (*e.g.* Hambrey & McKelvey 2000, Bart & Anderson 2000). The waxing and waning of the ice sheets resulted in strongly fluctuating IRD supply to the Southern Ocean (*e.g.* Ehrmann *et al.* 1991, Breza 1992, Cowan 2001, Murphy *et al.* 2002). However, even now, it is still a matter of debate, whether Antarctica was substantially deglaciated

during the mid-Pliocene warm period (Poore & Sloan 1996, Harwood & Webb 1998, Stroeven *et al.* 1998).

The alternations in depositional pattern on GR exhibit three prominent interglacials between 4.4 and 2.7 Ma. Considering possible stratigraphic inaccuracy as well as the low temporal resolution of the sampling intervals, we point out that the duration of one climatic cycle may come close to a period of 400 kyr, which corresponds to a Milankovitch parameter of eccentricity (e.g. Berger & Loutre 1991). However, as it was already stated for the late Miocene, the Antarctic ice sheets may not have changed in accordance with orbital frequencies before the onset of Northern Hemisphere glaciation (Barker *et al.* 1999, Barker & Camerlenghi 2002).

### Conclusions

- 1) Our study shows that the sediments of KMS and GR provide valuable information for reconstructing the Cenozoic palaeoenvironment, palaeoclimate and glacial history of Antarctica. The sediments exhumed at erosional features are therefore promising targets for further sediment sampling without the need for a drilling ship.
- 2) The investigated sediments cover the time intervals 30.1–29.0 Ma (early Oligocene), 14.1–12.8 Ma (middle Miocene), 8.8–6.5 Ma (late Miocene) and 5.1–2.7 Ma (Pliocene).
- 3) The Cenozoic sediments recovered on KMS and northern GR are dominated by siliceous oozes and siliceous muds implying deposition south of the Polar Front.
- 4) Icebergs reached the KMS and GR throughout the time represented by the investigated cores. However, the intensity of ice-rafting, as indicated by the amount of terrigenous sand, was very variable.
- 5) The clay mineral assemblages are dominated by illite and smectite, whereas chlorite and kaolinite occur only in traces. Illite and chlorite are derived from physical weathering of an East Antarctic source. Smectite and kaolinite probably are derived from the erosion of Cenozoic or Mesozoic shelf sediments. Kaolinite might also be supplied by AABW as a weathering product of Permo–Triassic sedimentary rocks eroded by ice streams draining into Prydz Bay.
- 6) The lower Oligocene sediments (30.1–29.0 Ma) indicate that most icebergs melted south of KMS and hydrographical properties of the water column favoured siliceous phytoplankton production. Palaeoenvironmental conditions on KMS were quite different from those on Maud Rise and Kerguelen Plateau, probably as a consequence of the separation of cold and warm surface water regimes by a coastal current. This leads to the assumption that in the Southern Ocean similar oceanographic features as today existed already at that time.
- 7) The sediments of the middle Miocene time interval 14.1–13.5 Ma point to similar palaeoenvironmental conditions as those of the early Oligocene. The diatom muds and oozes deposited between 13.5 and 13.1 Ma indicate relative warm conditions with a reduced glacial input of terrigenous detritus from the Antarctic continent in response to ice sheet retreat. The 13.1–12.8 Ma old sediments document major ice sheet build-up and an intensification of iceberg calving resulting in high concentrations of IRD.
- 8) Compared to the older sediments, the upper Miocene sediments (8.7–6.5 Ma) have higher contents of poorly crystallized and biotite-like illites and of IRD. This long-term change reflects continued cooling in Antarctica and the removal of smectite-enriched, kaolinite-bearing, pre-glacial sediments from the adjacent shelf and hinterland of GR and KMS. Superimposed short-term fluctuations in the sedimentological parameters point to a more dynamic Antarctic ice sheet.
- 9) The Pliocene sediments (5.1–2.7 Ma) show a pronounced episodic depositional pattern mirroring glacial and interglacial conditions. The duration of one climatic cycle may come close to about 400 kyr.

### Acknowledgements

W.E. collected the samples for this study during cruise ANT-VIII/6 of RV *Polarstern* and analysed them at the Alfred Wegener Institute for Polar and Marine Research in Bremerhaven. We thank the ship's master, crew and other cruise participants as well as the personnel at the institute for their support. The paper benefitted from the constructive reviews of Peter Barker, Angelo Camerlenghi and Christian Robert, and helpful comments of Alan Vaughan.

### References

- ABREU, V.S. & ANDERSON, J.B. 1998. Glacial eustasy during the Cenozoic: sequence stratigraphic implications. *American Association of Petroleum Geologists Bulletin*, **82**, 1385–1400.
- ANDERSON, J.B. 1999. *Antarctic marine geology*. Cambridge: Cambridge University Press, 289 pp.
- BARKER, P.F. & CAMERLENGHI, A. 2002. Glacial history of the Antarctic Peninsula from Pacific margin sediments. In BARKER, P.F., CAMERLENGHI, A., ACTON, G.D. & RAMSAY, A.T.S., eds. *Proceedings of the Ocean Drilling Program, Scientific Results*, **178**, 1–40.
- BARKER, P.F., BARRETT, P.J., COOPER, A.K. & HUYBRECHTS, P. 1999. Antarctic glacial history from numerical models and continental margin sediments. *Palaeogeography, Palaeoclimatology, Palaeoecology*, **150**, 247–267.

- BARKER, P.F., BARRETT, P.J., CAMERLENGHI, A., COOPER, A.K., DAVEY, F.J., DOMACK, E.W., ESCUTIA, C., KRISTOFFERSEN, Y. & O'BRIEN, P. 1998. Ice sheet history from Antarctic continental margin sediments: the ANTOSTRAT approach. *Terra Antarctica*, **5**, 737–760.
- BARKER, P.F., KENNETT, J.P. *et al.* 1988. *Proceedings of the Ocean Drilling Program, Initial Reports*, **113**, 785 pp.
- BARKER, P.F., KENNETT, J.P. *et al.* 1990. *Proceedings of the Ocean Drilling Program, Scientific Results*, **113**, 1033 pp.
- BARRETT, P.J., RICCI, C.A., DAVEY, F.J., EHRMANN, W., HAMBREY, M.J., JARRARD, R.D., VAN DER MEER, J.J.M., RAINE, J.I., ROBERTS, A.P., TALARICO, F. & WATKINS, D.K., *eds.* 2000a. Studies from the Cape Roberts Project, Ross Sea, Antarctica. Scientific Report of CRP-2/2A. Part I: Geophysics and physical properties, sedimentary environments. *Terra Antarctica*, **7**, 211–412.
- BARRETT, P.J., RICCI, C.A., DAVEY, F.J., EHRMANN, W., HAMBREY, M.J., JARRARD, R.D., VAN DER MEER, J.J.M., RAINE, J.I., ROBERTS, A.P., TALARICO, F. & WATKINS, D.K., *eds.* 2000b. Studies from the Cape Roberts Project, Ross Sea, Antarctica. Scientific Report of CRP-2/2A. Part II: Palaeontological studies, provenance and climate from petrology, chronology and chronostratigraphy. *Terra Antarctica*, **7**, 413–665.
- BARRETT, P.J., RICCI, C.A., BÜCKER, C.J., DAVEY, F.J., EHRMANN, W., LAIRD, M.G., VAN DER MEER, J.J.M., RAINE, J.I., SMELLIE, J.L., TALARICO, F., THOMSON, M.R.A., VEROSUB, K.L. & VILLA, G., *eds.* 2001a. Studies from the Cape Roberts Project, Ross Sea, Antarctica. Scientific Report of CRP-3. Part I: Geophysics and tectonic studies, sedimentary environments. *Terra Antarctica*, **8**, 119–308.
- BARRETT, P.J., RICCI, C.A., BÜCKER, C.J., DAVEY, F.J., EHRMANN, W., LAIRD, M.G., VAN DER MEER, J.J.M., RAINE, J.I., SMELLIE, J.L., TALARICO, F., THOMSON, M.R.A., VEROSUB, K.L. & VILLA, G., *eds.* 2001b. Studies from the Cape Roberts Project, Ross Sea, Antarctica. Scientific Report of CRP-3. Part II: Palaeontological studies, provenance and climate from petrology, chronology and chronostratigraphy. *Terra Antarctica*, **8**, 309–621.
- BARRON, J., LARSEN, B. *et al.* 1989. *Proceedings of the Ocean Drilling Program, Initial Reports*, **119**, 942 pp.
- BARRON, J., LARSEN, B. *et al.* 1991. *Proceedings of the Ocean Drilling Program, Scientific Results*, **119**, 1003 pp.
- BART, P.J. & ANDERSON, J.B. 2000. Relative temporal stability of the Antarctic ice sheets during the late Neogene based on the minimum frequency of outer shelf grounding events. *Earth and Planetary Science Letters*, **182**, 259–272.
- BARTEK, L.R., HENRYS, S.A., ANDERSON, J.B. & BARRETT, P.J. 1996. Seismic stratigraphy of McMurdo Sound, Antarctica: implications for glacially influenced early Cenozoic eustatic change? *Marine Geology*, **130**, 79–98.
- BERGER, A. & LOUTRE, M.F. 1991. Insolation values for the climate of the last 10 million years. *Quaternary Science Reviews*, **10**, 297–317.
- BERGGREN, W.A., KENT, D.V., SWISHER, C.C. & AUBRY, M.-P. 1995. A revised Cenozoic geochronology and chronostratigraphy. In BERGGREN, W.A., KENT, D.V., AUBRY, M.-P. & HARDENBOL, J., *eds.* *Geochronology, time scales and global stratigraphic correlation. SEPM Special Publications*, **54**, 129–212.
- BILLUPS, K. & SCHRAG, D.P. 2002. Paleotemperatures and ice volume of the past 27 Myr revisited with paired Mg/Ca and  $^{18}\text{O}/^{16}\text{O}$  measurements on benthic foraminifera. *Paleoceanography*, **17**, DOI 10.1029/2000PA000567.
- BISCAYE, P.E. 1964. Distinction between kaolinite and chlorite in recent sediments by X-ray diffraction. *American Mineralogist*, **49**, 1281–1289.
- BISCAYE, P.E. 1965. Mineralogy and sedimentation of recent deep-sea clay in the Atlantic Ocean and adjacent seas and oceans. *Geological Society of America Bulletin*, **76**, 803–832.
- BREZA, J.R. 1992. High-resolution study of Neogene ice-rafted debris, Site 751, Southern Kerguelen Plateau. In WISE JR, S.W., SCHLICH, R. *et al.*, *eds.* *Proceedings of the Ocean Drilling Program, Scientific Results*, **120**, 207–221.
- BRINDLEY, G.W. & BROWN, G., *eds.* 1980. Crystal structures of clay minerals and their X-ray identification. *Mineralogical Society Monograph*, **5**, 495 pp.
- BURCKLE, L.H. & CIRILLI, J. 1987. Origin of diatom ooze belt in the Southern Ocean: implications for late Quaternary palaeoceanography. *Micropaleontology*, **33**, 82–86.
- BURCKLE, L.H., MORTLOCK, R. & RUDOLPH, S. 1996. No evidence for extreme, long-term warming in early Pliocene sediments of the Southern Ocean. *Marine Micropaleontology*, **27**, 215–226.
- CISIELSKI, P.F., KRISTOFFERSEN, Y. *et al.* 1991. *Proceedings of the Ocean Drilling Program, Scientific Results*, **114**, 826 pp.
- COWAN, E.A. 2001. Identification of the glacial signal from the Antarctic Peninsula since 3.0 Ma at Site 1101 in a continental rise sediment drift. In BARKER, P.F., CAMERLENGHI, A., ACTON, G.D. & RAMSAY, A.T.S., *eds.* *Proceedings of the Ocean Drilling Program, Scientific Results*, **178**, 1–22 [CD-ROM]. Available from: Ocean Drilling Program, Texas A&M University, College Station, TX 77845-9547, USA.
- DIEKMANN, B. & KUHN, G. 1999. Provenance and dispersal of glacial-marine surface sediments in the Weddell Sea and adjoining areas, Antarctica: ice-rafting versus current transport. *Marine Geology*, **158**, 209–231.
- DIEKMANN, B., KUHN, G., MACKENSEN, A., PETSCHICK, R., FÜTTERER, D.K., GERSONDE, R., RÜHLEMANN, C. & NIEBLER, H.S. 1999. Kaolinite and chlorite as tracers of modern and late Quaternary deep water circulation in the South Atlantic and the adjoining Southern Ocean. In FISCHER, G. & WEFER, G., *eds.* *Use of proxies in paleoceanography: examples from the South Atlantic*. Berlin: Springer, 285–313.
- DIEKMANN, B., FÜTTERER, D.K., GROBE, H., HILLENBRAND, C.-D., KUHN, G., MICHELS, K., PETSCHICK, R. & PIRRUNG, M. In press. Terrigenous sediment supply in the polar to temperate South Atlantic: land–ocean links of environmental changes during the Late Quaternary. In WEFER, G., MULITZA, S. & RATMEYER, V., *eds.* *The South Atlantic in the Late Quaternary: reconstruction of material budget and current systems*. Berlin: Springer.
- DREWRY, D.J. 1986. *Glacial geological processes*. London: Arnold, 176 pp.
- EHRMANN, W.U. & MACKENSEN, A. 1992. Sedimentological evidence for the formation of an East Antarctic ice sheet in Eocene/Oligocene time. *Palaeogeography, Palaeoclimatology, Palaeoecology*, **93**, 85–112.
- EHRMANN, W.U., GROBE, H. & FÜTTERER, D.K. 1991. Late Miocene to Holocene glacial history of East Antarctica revealed by sediments from Sites 745 and 746. In BARRON, J., LARSEN, B. *et al.*, *eds.* *Proceedings of the Ocean Drilling Program, Scientific Results*, **119**, 239–260.
- EHRMANN, W.U., MELLES, M., KUHN, G. & GROBE, H. 1992. Significance of clay mineral assemblages in the Antarctic Ocean. *Marine Geology*, **107**, 249–273.
- EHRMANN, W., BLOEMENDAL, J., HAMBREY, M.J., MCKELVEY, B. & WHITEHEAD, J. 2003. Variations in the composition of the clay fraction of the Cenozoic Pagodroma Group, East Antarctica: implications for determining provenance. *Sedimentary Geology*, **161**, 131–152.
- EMERY, W.J. & MEINCKE, J. 1986. Global water masses: summary and review. *Oceanologica Acta*, **9**, 383–391.
- ESQUEVIN, J. 1969. Influence de la composition chimique des illites sur leur cristallinité. *Bulletin Centre Recherche Pau-SNPA*, **3**, 147–153.
- EXON, N.F., KENNETT, J.P., MALONE, M.J. *et al.* 2001. *Proceedings of the Ocean Drilling Program, Initial Reports*, **189**, [CD-ROM]. Available from: Ocean Drilling Program, Texas A&M University, College Station, TX 77845-9547, USA.
- FLOWER, B.J. & KENNETT, J.P. 1994. The middle Miocene climatic transition: East Antarctic ice sheet development, deep ocean circulation and global carbon cycling. *Palaeogeography, Palaeoclimatology, Palaeoecology*, **108**, 537–555.
- FÜTTERER, D.K. & SCHREMS, O., *eds.* 1991. The expedition ANTARKTIS-VIII of RV “Polarstern” 1989/90. Reports of Legs ANT-VIII/6-7. *Reports on Polar Research*, **90**, 231 pp.

- GERSONDE, R. & HODELL, D., eds. 2002. Southern Ocean paleoceanography - insights from Ocean Drilling Program Leg 177. *Palaeogeography, Palaeoclimatology, Palaeoecology*, **182**, 145–349.
- GERSONDE, R., SPIESS, V., FLORES, J.A., HAGEN, R.A. & KUHN, G. 1998. The sediments of Gunnerus Ridge and Kainan Maru Seamount (Indian sector of Southern Ocean). *Deep-Sea Research*, **45**, 1515–1540.
- GINGELE, F.X., KUHN, G., MAUS, B., MELLES, M. & SCHÖNE, T. 1997. Holocene ice retreat from the Lazarev Sea shelf, East Antarctica. *Continental Shelf Research*, **17**, 137–163.
- GROBE, H. & MACKENSEN, A. 1992. Late Quaternary climatic cycles as recorded in sediments from the Antarctic continental margin. *Antarctic Research Series*, **56**, 349–376.
- HAMBREY, M., WISE, S., BARRETT, P., DAVEY, F., EHRMANN, W., SMELLIE, J., VILLA, G. & WOOLFE, K., eds. 1998. Studies from the Cape Roberts Project, Ross Sea, Antarctica. Scientific Report of CRP-1. *Terra Antarctica*, **5**, 713 pp.
- HAMBREY, M.J. & MCKELVEY, B.C. 2000. Major Neogene fluctuations of the East Antarctic ice sheet: stratigraphic evidence from the Lambert Glacier region. *Geology*, **28**, 887–890.
- HARRIS, P.T. & O'BRIEN, P.E. 1998. Bottom currents, sedimentation and ice-sheet retreat facies successions on the Mac Robertson shelf, East Antarctica. *Marine Geology*, **151**, 47–72.
- HARWOOD, D.M. & WEBB, P.-N. 1998. Glacial transport of diatoms in the Antarctic Sirius Group: Pliocene refrigerator. *GSA Today*, **8**, 1–8.
- KENNETT, J.P. & BARKER, P.F. 1990. Latest Cretaceous to Cenozoic climate and oceanographic developments in the Weddell Sea, Antarctica: an ocean-drilling perspective. In BARKER, P.F., KENNETT, J.P. et al., eds. *Proceedings of the Ocean Drilling Program, Scientific Results*, **113**, 937–960.
- LATIMER, J.C. & FILIPPELLI, G.M. 2002. Eocene to Miocene terrigenous inputs and export production: geochemical evidence from ODP Leg 177, Site 1090. *Palaeogeography, Palaeoclimatology, Palaeoecology*, **182**, 151–164.
- LAWVER, L.A. & GAHAGAN, L.M. 2003. Evolution of Cenozoic seaways in the circum-Antarctic region. *Palaeogeography, Palaeoclimatology, Palaeoecology*, **198**, 11–37.
- LEAR, C.H., ELDERFIELD, H. & WILSON, P.A. 2000. Cenozoic deep-sea temperatures and global ice volumes from Mg/Ca in benthic foraminiferal calcite. *Science*, **287**, 269–272.
- MACKENSEN, A. & EHRMANN, W.U. 1992. Middle Eocene through Early Oligocene climate history and palaeoceanography in the Southern Ocean: stable oxygen and carbon isotopes from ODP Sites on Maud Rise and Kerguelen Plateau. *Marine Geology*, **108**, 1–27.
- MICHEL, K.H., KUHN, G., HILLENBRAND, C.-D., DIEKMANN, B., FÜTTERER, D.K., GROBE, H. & UENZELMANN-NEBEN, G. 2002. The southern Weddell Sea: combined contourite–turbidite sedimentation at the southeastern margin of the Weddell Gyre. In STOW, D.A.V., PUDSEY, C.J., HOWE, J.A., FAUGÈRES, J.-C. & VIANA, A.R., eds. *Deep-water Contourite Systems: modern drifts and characteristics*. *Geological Society Memoir*, **22**, 305–323.
- MURPHY, L., WARNKE, D.A., ANDERSSON, C., CHANNELL, J. & STONER, J. 2002. History of ice rafting at South Atlantic ODP Site 177-1092 during the Gauss and Late Gilbert Chrons. *Palaeogeography, Palaeoclimatology, Palaeoecology*, **182**, 183–196.
- O'BRIEN, P.E., COOPER, A.K., RICHTER, C. et al. 2001. *Proceedings of the Ocean Drilling Program, Initial Reports*, **188**, [CD-ROM]. Available from: Ocean Drilling Program, Texas A&M University, College Station, TX 77845-9547, USA.
- ORSI, A.H., NOWLIN JR, W.D. & WHITWORTH III, T. 1993. On the circulation and stratification of the Weddell Gyre. *Deep-Sea Research*, **40**, 169–203.
- ORSI, A.H., WHITWORTH III, T. & NOWLIN JR, W.D. 1995. On the meridional extent and fronts of the Antarctic Circumpolar Current. *Deep-Sea Research*, **42**, 641–673.
- ORSI, A.H., JOHNSON, G.C. & BULLISTER, J.L. 1999. Circulation, mixing, and production of Antarctic Bottom Water. *Progress in Oceanography*, **43**, 55–109.
- PAILLARD, D., LABEYRIE, L. & YIOU, P. 1996. Macintosh program performs time-series analysis. *Eos, Transactions, American Geophysical Union*, **77**, 379.
- POORE, R.Z. & SLOAN, L.C., eds. 1996. Introduction climates and climate variability of the Pliocene. *Marine Micropaleontology*, **27**, 1–326.
- PETSCHICK, R., KUHN, G. & GINGELE, F. 1996. Clay mineral distribution in surface sediments of the South Atlantic: sources, transport, and relation to oceanography. *Marine Geology*, **130**, 203–229.
- PUDSEY, C.J. 2002. The Weddell Sea: contourites and hemipelagites at the northern margin of the Weddell Gyre. In STOW, D.A.V., PUDSEY, C.J., HOWE, J.A., FAUGÈRES, J.-C. & VIANA, A.R., eds. *Deep-water Contourite Systems: modern drifts and ancient series, seismic and sedimentary characteristics*. *Geological Society Memoir*, **22**, 289–303.
- RAGUENEAU, O., TREGUER, P., LEYNAERT, A., ANDERSON, R.F., BRZEZINSKI, M.A., DEMASTER, D.J., DUGDALE, R.C., DYMOND, J., FISCHER, G., FRANCOIS, R., HEINZE, C., MAIER-REIMER, E., MARTIN-JEZEQUEL, V., NELSON, D.M. & QUEGUINER, B. 2000. A review of the Si cycle in the modern ocean: recent progress and missing gaps in the application of biogenic opal as a palaeoproductivity proxy. *Global and Planetary Change*, **26**, 317–365.
- ROBERT, C. & MAILLOT, H. 1990. Palaeoenvironments in the Weddell Sea area and Antarctic climates, as deduced from clay mineral associations and geochemical data, ODP Leg 113. In BARKER, P.F., KENNETT, J.P. et al., eds. *Proceedings of the Ocean Drilling Program, Scientific Results*, **113**, 51–66.
- ROBERT, C. & KENNETT, J.P. 1997. Antarctic continental weathering changes during the Eocene–Oligocene cryosphere expansion: clay mineral and oxygen isotope evidence. *Geology*, **25**, 587–590.
- ROESER, H.A., FRITSCH, J. & HINZ, K. 1996. The development of the crust off Dronning Maud Land, East Antarctica. In STOREY, B.C., KING, E.C. & LIVERMORE, R.A., eds. *Weddell Sea tectonics and Gondwana break-up*. *Geological Society Special Publication*, **108**, 243–264.
- SCHRÖDER, M. & FAHRBACH, E. 1999. On the structure and the transport of the eastern Weddell Gyre. *Deep-Sea Research II*, **46**, 501–527.
- STROEVEN, A., BURCKLE, L.H., KLEMAN, J. & PRENTICE, M.L. 1998. Atmospheric transport of diatoms in the Antarctic Sirius Group: Pliocene Deep Freeze. *GSA Today*, **8**, 1–5.
- TINGEY, R.J. 1991a. Commentary on schematic geological map of Antarctica Scale 1:10 000 000. *Bureau of Mineral Resources, Australia, Bulletin*, No. 238, 30 pp.
- TINGEY, R.J., ed. 1991b. *The geology of Antarctica*. Oxford: Clarendon Press, 650 pp.
- WARNKE, D.A., ALLEN, C.P., MÜLLER, D.W., HODELL, D.A. & BRUNNER, C. 1992. Miocene–Pliocene Antarctic glacial evolution: a synthesis of ice-rafted debris, stable isotope, and planktonic foraminiferal indicators, ODP Leg 114. *Antarctic Research Series*, **56**, 311–325.
- WEI, W. & WISE JR, S.W. 1990. Middle Eocene to Pleistocene calcareous nannofossils recovered by Ocean Drilling Program Leg 113 in the Weddell Sea. In BARKER, P.F., KENNETT, J.P. et al., eds. *Proceedings of the Ocean Drilling Program, Scientific Results*, **113**, 639–666.
- WHITWORTH III, T., ORSI, A.H., KIM, S.-J., NOWLIN JR, W.D. & LOCARNINI, R.A. 1998. Water masses and mixing near the Antarctic Slope Front. *Antarctic Research Series*, **75**, 1–27.
- WISE, S.W., BREZA, J.R., HARWOOD, D.M. & WEI, W. 1991. Palaeogene glacial history of Antarctica. In MÜLLER, D.W., MCKENZIE, J.A. & WEISSERT, H., eds. *Controversies in modern geology: evolution of geological theories in sedimentology, earth history and tectonics*. London: Academic Press, 133–171.
- ZACHOS, J., PAGANI, M., SLOAN, L., THOMAS, E. & BILLUPS, K. 2001. Trends, rhythms, and aberrations in global climate 65 Ma to present. *Science*, **292**, 686–693.